Hindawi
Mathematical Problems in Engineering
Volume 2020, Article ID 6207989, 13 pages
https://doi.org/10.1155/2020/6207989

Research Article

Energy Efficiency Optimization Algorithm of CR-NOMA System Based on SWIPT

Zhen Wang [1,2] **and Qi Zhu** [1,2]

[1]*Jiangsu Key Laboratory of Wireless Communications, Nanjing University of Posts and Telecommunications, Nanjing 210003, China*
[2]*Engineering Research Center of Health Service System Based on Ubiquitous Wireless Networks, Nanjing University of Posts and Telecommunications, Ministry of Education, Nanjing, China*

Correspondence should be addressed to Qi Zhu; zhuqi@njupt.edu.cn

Received 7 December 2019; Revised 16 May 2020; Accepted 1 June 2020; Published 29 June 2020

Academic Editor: José Domingo Álvarez

This paper proposes a system EE (energy efficiency) optimization algorithm based on OPS (On-off Power Splitting) strategy for SWIPT (Simultaneous Wireless Information and Power Transfer) two-way relay assisted CR-NOMA (Cognitive Radio Non-Orthogonal Multiple Access) network. The system capacity expression of the secondary users with the OPS strategy is derived. Under the constraints of harvested energy and quality of service (QoS) of the users, the optimization problem with the goal of maximizing energy efficiency is constructed. In this paper, the NP-Hard problem is transformed into three subproblems about relay power, NOMA coefficient, and segmentation coefficient, which are solved by golden section algorithm, monotonicity decision function, and genetic algorithm. The simulation results show that compared with the PS (Power Splitting) and TS (Time Switching) strategies, the OPS strategy can significantly improve the transmission energy efficiency of the system.

1. Introduction

Devices in energy-constrained wireless communication systems, such as wireless sensor networks, wireless positioning networks, and the Internet of Things are mostly battery-powered, and the limitations of battery-powered capacity and inconvenient replacement greatly limit the performance of the system [1]. Energy harvesting is an advanced technology that has emerged in recent years. By collecting renewable resources in the surrounding environment to provide nodes with the necessary working energy and extending the survival time of energy-constrained wireless networks, the goal of achieving green communications is achieved [2]. In addition to harvesting energy from renewable energy sources such as solar energy, wind energy, and geothermal energy, there are near-field power transmission using inductive, capacitive, or resonant coupling, and far-field wireless power transmission via RF (radio frequency), wireless powering of devices using near-field Inductive Power Transfer, has become a reality with several commercially available products and standards. However, its range is severely limited (less than one meter). On the other hand, far-field Wireless Power Transfer (WPT) via RF (as in wireless communication) could be used over longer ranges, which is the main focus of this paper [3]. Due to the advantages of low cost and stable power, WPT will be widely used in the Internet of Things and various types of mobile terminals and has attracted widespread attention in the academic and industrial circles.

SWIPT is a product of the combination of wireless energy transmission and wireless information transmission (WIT), which can realize energy harvesting and information transmission at the same time. Nasir et al. [4] proposed two energy harvesting strategies for time switching and power splitting for energy harvesting relay networks and derived the throughput expression of the system. Nasir et al. [5] proposed continuous time acquisition strategy and discrete time acquisition strategy for TS strategy and compared the system outage probability of the two strategies by analyzing the probability of system interruption. Zhou et al. [6] designed a universal receiver that separates the received signals with adjustable power ratios for energy harvesting

and information decoding and derives the rate-energy ratio of time switching, static power splitting, and on-off power splitting. Huang and Larsson [7] proposed a power control algorithm for SWIPT-based Orthogonal Frequency Division Multiplex (OFDM) networks to optimize system throughput in this scenario. Zhou et al. [8] studied the design of the SWIPT acquisition strategy in the downlink multiuser OFDM system; TS was used at the receiver for time-division multiplexed information transmission; PS was used at the receiver for OFDM-based information transmission, and the segmentation coefficients of the two strategies are optimized.

NOMA allows multiple users to share the same channel resources in the same cell at the same time, which makes it possible to obtain higher spectral efficiency than traditional orthogonal multiple access (OMA) technology. Zaidi et al. [9] deduced the expressions of user's outage probability and system throughput for the NOMA system based on SWIPT to evaluate the performance of the system. Bariah et al. [10] deduced the bit error rate expression of all users under PS strategy for the cooperative relay NOMA network based on SWIPT. Tang et al. [11] aimed at the joint power allocation problem in the NOMA system based on PS strategy. In order to simplify the problem, the energy harvested by the user was converted into the throughput, and the sum of the converted throughput and the user's transmission rate was defined as the new objective function, so [11] can give the optimization algorithm for user power and segmentation coefficient. Hedayati and Kim [12] aimed at the joint power allocation problem in the SWIPT-NOMA system based on the TS strategy and proposed an energy efficiency optimization algorithm that satisfies the requirements of transmit power limit, harvested energy, and quality of service. Tang [13] aimed at the joint power allocation problem in the SWIPT-NOMA system based on the TS strategy and proposed an energy efficiency optimization algorithm that satisfies the requirements of transmit power limit, harvested energy, and quality of service. Chang [14] investigated resource allocation algorithm design for an OFDM-based NOMA system empowered by wireless power transfer. Jameel [15] employed deep learning-based optimization to solve the problem of power distribution in SWIPT-NOMA network.

Cognitive radio technology can improve the spectrum utilization of the system by sharing the spectrum between different systems. In [16], a closed-form expression of the outage probability was derived for CR-NOMA networks based on SWIPT. Yang et al. [17] aimed at the SWIPT-based NOMA network, respectively, under the two strategies of fixed allocation and optimized allocation of the NOMA coefficient, and the user's outage probability was derived. Wang [18] derived the approximate expression of energy efficiency based on SWIPT-based CR-NOMA system and gave the relay power and time slot allocation scheme with the energy efficiency maximization as the optimization goal. Zhao et al. [19] proposed a two-way relay CR-NOMA system based on PS strategy and gave an optimization algorithm with energy efficiency as the optimization goal under the constraints of harvested energy and quality of service, but it did not consider the two typical strategies of TS and OPS.

This paper proposes a system energy efficiency optimization algorithm using the OPS strategy for a two-way relay CR-NOMA system based on SWIPT. The main innovations of this paper are as follows:

(i) The system capacity expressions with the TS strategy and the OPS strategy are derived, respectively. Under the constraints of harvested energy and quality of service, an optimization problem with the goal of maximizing energy efficiency is constructed.

(ii) The objective function is a multiobjective optimized NP-Hard problem. In this paper, the original problem is transformed into three subproblems about relay power, NOMA coefficient, and segmentation coefficient, which are solved by the golden section algorithm, the monotonicity determination method of the function, and the genetic algorithm; then, the solutions of three subproblems are jointly optimized by alternating iterative algorithm.

(iii) The simulation results show that compared with the PS and TS strategies, the OPS strategy can significantly improve the transmission energy efficiency of the system. Since the OPS strategy can control time division and power division at the same time, thereby ensuring that the system completes the communication process with the lowest energy requirements, OPS strategy is better than PS and TS strategy when the power limit of different users and the distance between the near user and the relay are different.

The following content of this article is arranged as follows. The system model of the SWIPT-based two-way relay assisted CR-NOMA network is presented in Section 2. We describe the optimization problem with the goal of maximizing energy efficiency and give the optimization algorithm in Section 3. The simulation results and analyses are given in Section 4. Finally, we draw our conclusions in Section 5.

2. System Model

The system model of a two-way relay assisted CR-NOMA system in this paper is shown in Figure 1 [19], which includes a primary transmitter (PT), a primary receiver (PR), a two-way relay (TWR), and four secondary users of RF energy harvesting ability, among them, SU1 and SU3 and SU2 and SU4 are each a pair of sending and receiving users, and SU1 and SU3 are closer to TWR and SU3 and SU4 are farther from TWR.

The communication process of the system is divided into two phases. In the first phase, four secondary users send signals to TWR at the same time. TWR receives and decodes the mixed signal in turn, which is subject to interference from the primary transmitter. In the second phase, TWR forwards the superimposed signals $\sqrt{b_1 P_r}x_1 + \sqrt{b_2 P_r}x_2$ and $\sqrt{b_3 P_r}x_3 + \sqrt{b_4 P_r}x_4$ to the two sets of NOMA secondary users SU1 and SU2 and SU3 and SU4 with a transmit power of P_r and causes interference to the primary receiver, where x_i is the signal that TWR forwards to the secondary user SUi and b_i is the power allocation coefficient in NOMA. Because SU2

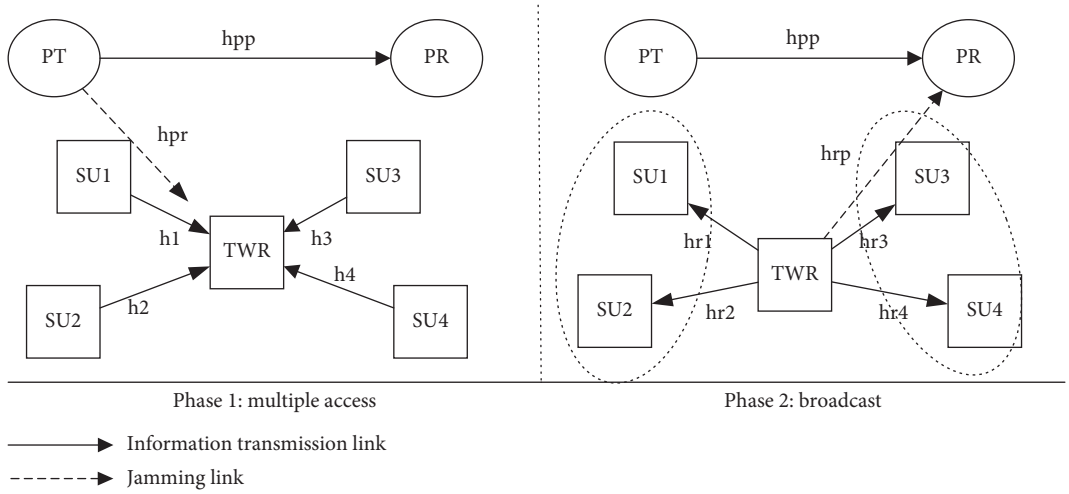

Figure 1: System model of two-way relay CR-NOMA.

and SU4 are remote users, in order to ensure the fairness of NOMA, $b_1 < b_2$ and $b_3 < b_4$, which means x_1 and x_3 are weak signals and x_2 and x_4 are strong signals. In the second phase, the secondary user receives and decodes the superimposed signal forwarded by the TWR, which completes the collection of the RF signal energy sent by the TWR at the same time. Channel state information (CSI) is assumed to be perfectly known at all terminals. Note that the CSI at the receivers can be obtained from the channel estimation of the downlink pilots, while CSI at the transmitter can be acquired via uplink channel estimation in the TDD mode [13].

2.1. Time Switching. The system model of TS is shown in Figure 2, where the front $(1-\lambda)T/2$ is the first phase, and the rest is the second phase, and T is the length of a communication process of the system. TS realizes two processes of energy collection and information transmission by dividing time, namely, energy harvesting is completed during the front λT and information transmission is completed during the rear $(1-\lambda)T/2$.

For ease of calculation, it is assumed that the channel gains of the two groups of users are completely symmetrical. We take SU1 and SU2 as examples, the received signals and harvested energy are given by

$$\begin{aligned} y_i^{TS} &= h_{Ri}\left(\sqrt{b_1 P_r}\, x_1 + \sqrt{b_2 P_r}\, x_2\right) + n_i, \\ E_i^{TS} &= \eta\lambda P_r \left|h_{Ri}\right|^2 T, \end{aligned} \tag{1}$$

where h_{Ri} is the link channel gain from TWR, η is the efficiency of energy collection, n_i is Gaussian white noise (AWGN) at SUi, and the power is σ^2. In practice, EH circuits usually result in a nonlinear end-to-end wireless power transfer [20, 21], and for the convenience of calculation, according to [13, 19], this paper assumes power conversion efficiency is independent of the input power level of the EH circuit and employs a linear energy harvesting model.

SU1 is a near user and needs to decode the strong signal first and then the weak signal required. The information rates of the two signals are given by

$$\begin{aligned} R_{1\longrightarrow 2}^{TS} &= \frac{1-\lambda}{2}\log_2\left(1 + \frac{b_2 P_r \left|h_{R1}\right|^2}{\sigma^2 + b_1 P_r \left|h_{R1}\right|^2}\right), \\ R_1^{TS} &= \frac{1-\lambda}{2}\log_2\left(1 + \frac{b_1 P_r}{\sigma^2}\left|h_{Ri}\right|^2\right). \end{aligned} \tag{2}$$

SU2 can directly decode the required strong signal, and its rate is expressed as follows:

$$R_2^{TS} = \frac{1-\lambda}{2}\log_2\left(1 + \frac{b_2 P_r \left|h_{R2}\right|^2}{\sigma^2 + b_1 P_r \left|h_{R2}\right|^2}\right). \tag{3}$$

All the energy harvested by the secondary users is used to complete the signal transmission in the first phase. The maximum average transmission power is obtained by

$$P_i^{TS} = \frac{E_i^{TS}}{1-\lambda/2T} = \frac{2\lambda}{1-\lambda}\eta P_r \left|h_{Ri}\right|^2. \tag{4}$$

The signal rate received by the primary receiver in the second phase is given by

$$R_p^{TS} = \frac{1-\lambda}{2}\log_2\left(1 + \frac{P_t \left|h_{PP}\right|^2}{P_r \left|h_{RP}\right|^2 + \sigma_P^2}\right), \tag{5}$$

where h_{RP} and h_{PP} are the channel gains between TWR and PR and the primary transmitter and primary receiver in the second phase, respectively, and n_p is Gaussian white noise at the primary receiver in the second phase, its power is σ_P^2.

2.2. On-Off Power Splitting. The system model of OPS is shown in Figure 3. The division of time slots is the same as that of TS, the first $(1-\lambda)T/2$ is the first phase, and the rest is the second phase; the difference is that OPS combines the characteristics of PS. During the rear $(1-\lambda)T/2$ in the second phase, OPS divides P_r into two parts ρP_r and $(1-\rho)P_r$; ρP_r is used for energy harvesting and $(1-\rho)P_r$ is used to complete the information transmission between TWR and SU.

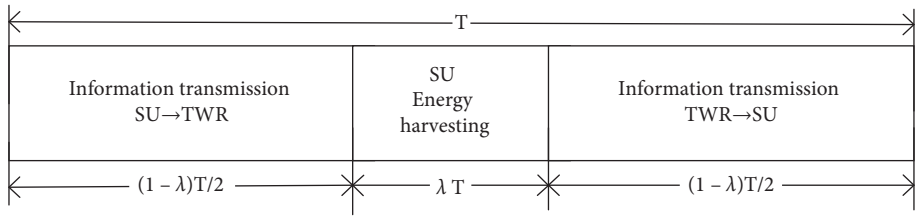

Figure 2: System model of time switching.

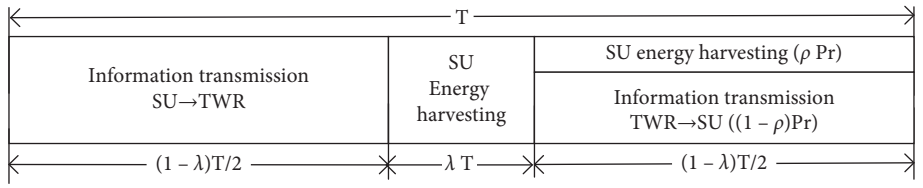

Figure 3: System model of on-off power splitting.

The signals received by the secondary users and the energy harvested are given by

$$y_i^{OPS} = \sqrt{1-\rho}h_{Ri}\left(\sqrt{b_1P_r}\,x_1 + \sqrt{b_2P_r}\,x_2\right) + n_i,$$
$$E_i^{OPS} = \left(\lambda + \frac{\rho(1-\lambda)}{2}\right)\eta P_r\left|h_{Ri}\right|^2 T. \tag{6}$$

The information rates of the strong and weak signals at SU1 are obtained by

$$R_{1\longrightarrow 2}^{OPS} = \frac{1-\lambda}{2}\log_2\left(1 + \frac{(1-\rho)b_2P_r\left|h_{R1}\right|^2}{\sigma^2 + (1-\rho)b_1P_r\left|h_{R1}\right|^2}\right),$$
$$R_1^{OPS} = \frac{1-\lambda}{2}\log_2\left(1 + \frac{(1-\rho)b_1P_r\left|h_{R1}\right|^2}{\sigma^2}\right). \tag{7}$$

The strong signal information rate at SU2 is expressed as follows:

$$R_2^{OPS} = \frac{1-\lambda}{2}\log_2\left(1 + \frac{(1-\rho)b_2P_r\left|h_{R2}\right|^2}{\sigma^2 + (1-\rho)b_1P_r\left|h_{R2}\right|^2}\right). \tag{8}$$

The maximum transmit power of the secondary user is given by

$$P_i^{OPS} = \frac{E_i^{OPS}}{1-\lambda/2T} = \left(\frac{2\lambda}{1-\lambda} + \rho\right)\eta P_r\left|h_{Ri}\right|^2. \tag{9}$$

The information rate of the primary receiver is the same as the rate under the TS strategy, which is given by

$$R_p^{OPS} = R_p^{TS} = \frac{1-\lambda}{2}\log_2\left(1 + \frac{P_t\left|h_{PP}\right|^2}{P_r\left|h_{RP}\right|^2 + \sigma_P^2}\right). \tag{10}$$

3. Problem Formulation

Assume that the channel gains of the two groups of users are completely symmetrical, that is, $h_{R1} = h_{R3}$ and $h_{R2} = h_{R4}$, and the system capacity is the sum of the information rates of the four secondary users, which is given by

$$R_{tot} = 2\left(R_1 + R_2\right). \tag{11}$$

Define the energy consumption of the system as the difference between the energy consumed by the system and the energy collected by the secondary user, which is expressed as follows:

$$E_{tot} = P_lT + P_rT_2 - 2\left(E_1 + E_2\right), \tag{12}$$

where T_2 is the length of the second phase and P_l is the circuit power loss.

This paper needs to maximize the energy efficiency of the system by optimizing the relay power, the NOMA coefficient, and the division coefficient. The optimization problem can be expressed as follows:

$$\begin{aligned}
\max_{P_r,b_3,\rho,\lambda}\quad & \eta_{EE} = \frac{R_{tot}}{E_{tot}} \\
\text{s.t.}\quad & R_P \geq i_{th} \\
& R_{1\longrightarrow 2} \geq r_{th} \\
& P_{tot} \geq P_s \\
& P_r \leq P_{\max} \\
& 0 \leq \rho \leq 1, 0 \leq \lambda \leq 1 \\
& 0 \leq b_1 \leq 0.5, b_2 = 1 - b_1.
\end{aligned} \tag{13}$$

Among them, i_{th} is the information rate threshold of the primary receiver, r_{th} is the minimum information rate that satisfies the signal-to-interference-and-noise ratio of the strong signals decoded by SU1 and SU3, $P_{\max}$ is the maximum threshold of the relay transmission power, and P_{tot} is the sum of the transmission power of the secondary users, its threshold is P_s.

This problem is a multivariable optimized NP-Hard problem, which has high complexity and cannot be solved directly. As stated in [22], for any optimization problems with multiple variables, we can analyze and solve the problem over some variables, regarding the rest as constants; then, solve the problem over the remaining variables. Therefore, we will separate P_r, b_3, and ρ or λ when developing the optimization algorithm so as to overcome the difficulty. Furthermore, this paper decomposes it into three optimization subproblems about relay power, NOMA coefficient, and partition coefficient, regarding the remaining variables as constants when solving the suboptimization problem of each variable, which are obtained by

$$\begin{aligned} \text{SP1:}\quad & \max_{P_r} \quad \eta_{EE} = \frac{R_{tot}}{E_{tot}} \\ & \text{s.t.} \quad R_P \geq i_{th} \\ & \qquad R_{1\longrightarrow 2} \geq r_{th} \\ & \qquad P_{tot} \geq P_s \\ & \qquad P_r \leq P_{\max}, \end{aligned} \tag{14}$$

$$\begin{aligned} \text{SP2:}\quad & \max_{b_1} \quad \eta_{EE} = \frac{R_{tot}}{E_{tot}} \\ & \text{s.t.} \quad R_{1\longrightarrow 2} \geq r_{th} \\ & \qquad 0 \leq b_1 \leq 0.5, \end{aligned} \tag{15}$$

$$\begin{aligned} \text{SP3:}\quad & \max_{\rho,\lambda} \quad \eta_{EE} = \frac{R_{tot}}{E_{tot}} \\ & \text{s.t.} \quad R_P \geq i_{th} \\ & \qquad R_{1\longrightarrow 2} \geq r_{th} \\ & \qquad P_{tot} \geq P_s \\ & \qquad 0 \leq \rho, \lambda \leq 1. \end{aligned} \tag{16}$$

3.1. Optimization of TWR Transmission Power. Because the expressions of η_{EE}, R_P, $R_{1\longrightarrow 2}$, and P_{tot} of the TS and OPS strategies are inconsistent, the constraints and objective functions of P_r for both strategies will be given separately:

$$\max_{P_r} \eta_{EE}^{TS} = \frac{(1-\lambda)\log_2\left(1 + b_1 P_r |h_{R1}|^2/\sigma^2\right) + (1-\lambda)\log_2\left(1 + b_2 P_r |h_{R2}|^2/\sigma^2 + b_1 P_r |h_{R2}|^2\right)}{P_l T + P_r((1+\lambda)/2)T - 2\lambda\eta P_r\left(|h_{R1}|^2 + |h_{R2}|^2\right)T},$$

$$\begin{cases} \dfrac{1-\lambda}{2}\log_2\left(1 + \dfrac{P_t |h_{PP}|^2}{P_r |h_{RP}|^2 + \sigma_P^2}\right) \geq i_{th}, \\ \dfrac{1-\lambda}{2}\log_2\left(1 + \dfrac{b_2 P_r |h_{R1}|^2}{\sigma^2 + b_1 P_r |h_{R1}|^2}\right) \geq r_{th}, \\ \dfrac{4\lambda}{1-\lambda}\eta P_r\left(|h_{R1}|^2 + |h_{R2}|^2\right) \geq P_s, \\ P_r \leq P_{\max}, \end{cases} \tag{17}$$

$$\max_{P_r} \eta_{EE}^{OPS} = \frac{(1-\lambda)\log_2\left(1 + (1-\rho) b_1 P_r |h_{R1}|^2/\sigma^2\right) + (1-\lambda)\log_2\left(1 + (1-\rho) b_2 P_r |h_{R2}|^2/\sigma^2 + (1-\rho) b_1 P_r |h_{R2}|^2\right)}{P_l T + P_r((1+\lambda)/2)T - 2\lambda\eta P_r\left(|h_{R1}|^2 + |h_{R2}|^2\right)T - (1-\lambda)\rho\eta P_r\left(|h_{R1}|^2 + |h_{R2}|^2\right)T},$$

$$\begin{cases} \dfrac{1-\lambda}{2}\log_2\left(1 + \dfrac{P_t |h_{PP}|^2}{P_r |h_{RP}|^2 + \sigma_P^2}\right) \geq i_{th}, \\ \dfrac{1-\lambda}{2}\log_2\left(1 + \dfrac{(1-\rho) b_2 P_r |h_{R1}|^2}{\sigma^2 + (1-\rho) b_1 P_r |h_{R1}|^2}\right) \geq r_{th}, \\ \left(\dfrac{4\lambda}{1-\lambda} + 2\rho\right)\eta P_r\left(|h_{R1}|^2 + |h_{R2}|^2\right) \geq P_s, \\ P_r \leq P_{\max}. \end{cases}$$

The fractional objective function makes the problem neither linear nor convex and thus difficult to solve straightforwardly. By analyzing the objective function, this paper gets the following proposition.

Proposition 1. *The objective function in equation (14) is strictly quasi-concave function in the TWR transmission power P_r.*

Proof. Take the objective function of TS strategy as an example, and its objective function can be written as follows:

$$\begin{aligned}\eta_{EE}(P_r) &= \frac{(1-\lambda)\left(\log_2\left(1+b_1P_r\left|h_{R1}\right|^2/\sigma^2\right)+\log_2\left(1+b_2P_r\left|h_{R2}\right|^2/\sigma^2+b_1P_r\left|h_{R2}\right|^2\right)\right)}{\left((1+\lambda/2)T-2\lambda\eta\left(\left|h_{R1}\right|^2+\left|h_{R2}\right|^2\right)T\right)P_r+P_lT} \\ &= \frac{F_U(P_r)}{F_L(P_r)}.\end{aligned} \tag{18}$$

Since the remaining variables are all considered constant at this time, $F_L(P_r)$ is a linear function with respect to P_r. $F_U(P_r)$ is the concave function of P_r, to prove that, the second-order partial derivative of $F_U(P_r)$ with respect to P_r is required. The first-order partial derivative of $F_U(P_r)$ can be denoted as follows:

$$\text{TS: } \frac{\partial F_U(P_r)}{\partial P_r} = \frac{1-\lambda}{\ln 2}\left(\frac{b_1\left|h_{R1}\right|^2}{\sigma^2+b_1P_r\left|h_{R1}\right|^2}+\frac{\left|h_{R2}\right|^2}{\sigma^2+P_r\left|h_{R2}\right|^2}-\frac{b_1\left|h_{R2}\right|^2}{\sigma^2+b_1P_r\left|h_{R2}\right|^2}\right). \tag{19}$$

Furthermore, the second-order partial derivative of $F_U(P_r)$ can be obtained as follows:

$$\begin{aligned}\text{TS: } \frac{\partial^2 F_U(P_r)}{\partial P_r^2} &= \frac{1-\lambda}{\ln 2}\left(-\frac{\left(b_1\left|h_{R1}\right|^2\right)^2}{\left(\sigma^2+b_1P_r\left|h_{R1}\right|^2\right)^2}-\frac{\left|h_{R2}\right|^4}{\left(\sigma^2+P_r\left|h_{R2}\right|^2\right)^2}+\frac{\left(b_1\left|h_{R2}\right|^2\right)^2}{\left(\sigma^2+b_1P_r\left|h_{R2}\right|^2\right)^2}\right) \\ &= \frac{1-\lambda}{\ln 2}\left(\left(\frac{1}{\left(\left(\sigma^2/b_1\left|h_{R2}\right|^2\right)+1\right)^2}-\frac{1}{\left(\left(\sigma^2/b_1\left|h_{R1}\right|^2\right)+1\right)^2}\right)-\frac{\left|h_{R2}\right|^4}{\left(\sigma^2+P_r\left|h_{R2}\right|^2\right)^2}\right).\end{aligned} \tag{20}$$

Since $|h_{R1}|^2 > |h_{R2}|^2$, the right side of the equation is all negative, $\partial^2 F_U(P_r)/\partial P_r^2 < 0$. Thus, $F_U(P_r)$ is the concave function with respect to P_r. Therefore, the objective function is strictly quasi-concave function for P_r [22]. Furthermore, this paper can prove that the objective function is first monotonically nonincrease and then monotonically nondecrease. The proof can be easily obtained by $\partial\eta_{EE}(P_r)/\partial P_r|_{P_r\longrightarrow 0} \le 0$ and $\partial\eta_{EE}(P_r)/\partial P_r|_{P_r\longrightarrow\infty} > 0$ [23]. The process of proving the OPS strategy is similar to the above process and is omitted here.

According to Proposition 1, an unique global optimal solution exists and the optimal point can be obtained by using the bisection method [22]. Since the Dinkelbach method [24] has been widely applied to solve nonlinear fractional optimization problem, we apply it to tackle our EE maximization problem. Particularly, we convert the fractional objective function into a subtractive form of numerator and denominator on the basis of the following proposition.

Proposition 2. *For $F_U(P_r) \ge 0$ and $F_L(P_r) \ge 0$, the maximum achievable EE $q^* = \eta_{EE}^*$ satisfies the following equation:*

$$\max_{P_r\ge 0} F_U(P_r) - q^*F_L(P_r) = F_U(P_r^*) - q^*F_L(P_r^*) = 0, \tag{21}$$

Table 1: Golden section algorithm for optimal relay power.

Algorithm: golden section algorithm of optimal relay power
1. Initialize the remaining variables and constant terms $\eta = 80\%$, $b_1 = 0.5$, $\lambda^{TS} = 0.3$, $\lambda^{OPS} = 0.2$, $\rho^{PS} = 0.5$, $\rho^{OPS} = 0.5$, $T = 1$.
2. Determine tolerance δ, $\beta = 0.618$, $\alpha = 0.382$, the initial interval is $[a, b]$, where $a = \max(\chi_1, \chi_2)$, $b = \min(\chi_3, P_{\max})$.
3. While $b - a > \delta$:
4. $t_1 = a + \alpha(b-a)$, $t_2 = a + \beta(b-a)$, $\eta_{EE}^1 = \eta_{EE}(t_1)$, $\eta_{EE}^2 = \eta_{EE}(t_2)$.
5. If $\eta_{EE}(t_2) < \eta_{EE}(t_1)$, then $b = t_2$, $t_2 = t_1$, $\eta_{EE}(t_2) = \eta_{EE}(t_1)$, $t_1 = \alpha + \alpha(b-a)$, $\eta_{EE}^1 = \eta_{EE}(t_1)$,
6. Else $a = t_1$, $t_1 = t_2$, $\eta_{EE}(t_1) = \eta_{EE}(t_2)$, $t_2 = \alpha + \beta(b-a)$, $\eta_{EE}^2 = \eta_{EE}(t_2)$,
7. End, $t^* = t_1 + t_2/2$.
8. The optimal value t^* is the optimal relay power P_r^* that meets the maximum energy efficiency.

where $F_U(P_r)$ is the numerator of the objective function, $F_L(P_r)$ is the denominator of the objective function, and $q^* = F_U(P_r^*)/F_L(P_r^*)$.

Proof. Please refer to [24] for the proof of Proposition 1.

Proposition 2 shows that the original complex fractional objective function can be transformed into an equivalent optimization problem with subtraction. After such a transformation, this paper presents an algorithm to solve the equivalent optimization problem that satisfies the conditions in Proposition 1, which can be concluded in Table 1.

In order to ensure the feasibility of the algorithm in Table 2, it is necessary to prove its convergence. First, this paper proves that $q^{(n)}$ will increase in each iteration. Note that q^* satisfies the optimal condition in Proposition 2, i.e., $F_U(P_r^*) - q^* F_L(P_r^*) = \varphi(q^*) = 0$. Suppose that $P_r^{(n)}$ is the optimal power allocation, n is the number of iterations, and $q^{(n)} \neq q^*$ and $q^{(n+1)} \neq q^*$ represent the corresponding optimal energy efficiency. It has been proved in [23] that $\varphi(q^{(n)}) > 0$ and $\varphi(q^{(n+1)}) > 0$ hold. In addition, in the algorithm of Table 2, $q^{(n+1)} = F_U(P_r^{(n)})/F_L(P_r^{(n)})$. So, this article can obtain the following expression:

$$\begin{aligned}\varphi\left(q^{(n)}\right) &= F_U\left(P_r^{(n)}\right) - q^{(n)} F_L\left(P_r^{(n)}\right) \\ &= q^{(n+1)} F_L\left(P_r^{(n)}\right) - q^{(n)} F_L\left(P_r^{(n)}\right) \\ &= \left(q^{(n+1)} - q^{(n)}\right) F_L\left(P_r^{(n)}\right).\end{aligned} \tag{22}$$

Since $F_L(P_r^{(n)})$ represents the energy consumed, there is always $F_L(P_r^{(n)}) > 0$, so $q^{(n+1)} > q^{(n)}$. Then, we prove that $q^{(n)}$ converges to the optimal value q^* if the number of iterations is large enough. Since there is a limit value q^* and $q^{(n)}$ will increase every iteration, when the number of iterations n is large enough, $q^{(n+1)} \longrightarrow q^{(n)}$ and $\varphi(q^{(n+1)}) \longrightarrow 0$ hold, and the optimality condition in Proposition 1 can be met.

After the above proof, the suboptimization problem SP1 can be converted into the following equation:

Table 2: Iterative algorithm based on the Dinkelbach method.

Algorithm: iterative algorithm based on the Dinkelbach method
1. Initialize $n = 0$, $P_r^{(n)} = 1$ and $q^{(n)} = 0$, set the stopping criterion ε;
2. While $F_U(P_r^{(n)}) - q^{(n)} F_L(P_r^{(n)}) > \varepsilon$
3. For given $q^{(n)}$, solve (20) to obtain the transmission power $P_r^{(n)}$;
4. Let $n = n + 1$ and $q^{(n)} = F_U(P_r^{(n-1)})/F_L(P_r^{(n-1)})$;
5. The optimal energy efficiency $\eta_{EE}^* = q^*$ is $q^{(n)}$.

$$\begin{aligned}&\max_{P_r} F_U(P_r) - qF_L(P_r), \\ &\max(\chi_1, \chi_2) \le P_r \le \min(\chi_3, P_{\max}), \\ &\begin{cases} \chi_1^{TS} = \dfrac{\sigma^2 R_{th}^{TS}}{b_2 |h_{R1}|^2 - b_1 R_{th}^{TS} |h_{R1}|^2}, \\ \chi_2^{TS} = \dfrac{(1-\lambda) P_s}{4\lambda\eta\left(|h_{R1}|^2 + |h_{R2}|^2\right)}, \\ \chi_3^{TS} = \dfrac{P_t |h_{PP}|^2 - \sigma_p^2 I_{th}^{TS}}{|h_{RP}|^2 I_{th}^{TS}}, \end{cases} \\ &\begin{cases} \chi_1^{OPS} = \dfrac{\sigma^2 R_{th}^{OPS}}{(1-\rho)\left(b_2 |h_{R1}|^2 - b_1 R_{th}^{OPS} |h_{R1}|^2\right)}, \\ \chi_2^{OPS} = \dfrac{(1-\lambda) P_s}{(4\lambda + (2-2\lambda)\rho)\eta\left(|h_{R1}|^2 + |h_{R2}|^2\right)}, \\ \chi_3^{OPS} = \dfrac{P_t |h_{PP}|^2 - \sigma_p^2 I_{th}^{OPS}}{|h_{RP}|^2 I_{th}^{OPS}}, \end{cases} \end{aligned} \tag{23}$$

where $R_{th}^{OPS} = R_{th}^{TS} = 2^{2r_{th}/(1-\lambda)} - 1$ and $I_{th}^{OPS} = I_{th}^{TS} = 2^{2i_{th}/(1-\lambda)} - 1$.

Considering the remaining two variables as constants, the original problem becomes a problem of finding the

maximum value in the specified interval. This paper uses the golden section algorithm to find the optimal relay power. However, the golden section method can only be used to solve the extreme points in the single-peak interval. Therefore, it is necessary to prove that the objective function is a convex function.

According to Proposition 1, $F_U(P_r)$ is the concave function with respect to P_r. Since $F_L(P_r)$ is a linear function of P_r, its second-order partial derivative is 0. Therefore, the positive and negative properties of the second derivative of $F_U(P_r) - qF_L(P_r)$ are consistent with $F_U(P_r)$. We can conclude that, for a fixed parameter q, the transformation form of objective function $F_U(P_r) - qF_L(P_r)$ is strictly concave in P_r.

After proving that the objective function is a concave function, this paper can use the golden section algorithm to satisfy the value of P_r with the greatest energy efficiency. The specific algorithm steps are shown in Table 1.

3.2. Optimization of NOMA Coefficient. In SP2, b_1 is included only in the R_{tot} term, so the original question SP2 can be simplified as follows:

$$\begin{aligned} \max_{b_1} \quad & R_{tot} \\ \text{s.t.} \quad & R_{1\longrightarrow 2} \geq r_{th} \\ & 0 \leq b_1 \leq 0.5. \end{aligned} \tag{24}$$

We simplify R_{tot} according to $b_1 + b_2 = 1$ and take R_{tot}^{OPS} as an example, which is given by

$$\begin{aligned} R_{tot}^{OPS} &= (1-\lambda)\log_2\left(1 + \frac{(1-\rho)b_1 P_r |h_{R1}|^2}{\sigma^2}\right) + (1-\lambda)\log_2\left(1 + \frac{(1-\rho)b_2 P_r |h_{R2}|^2}{\sigma^2 + (1-\rho)b_1 P_r |h_{R2}|^2}\right), \\ &= (1-\lambda)\log_2\left(\sigma^2 + (1-\rho)b_1 P_r |h_{R1}|^2\right) - (1-\lambda)\log_2\left(\sigma^2 + (1-\rho)b_1 P_r |h_{R2}|^2\right) \\ &\quad - (1-\lambda)\log_2\left(\sigma^2\right) + (1-\lambda)\log_2\left(\sigma^2 + (1-\rho)P_r |h_{R2}|^2\right). \end{aligned} \tag{25}$$

Since the last term in equation (25) is a constant term independent of b_1, the partial derivative of R_{tot}^{OPS} for b_1 is expressed as follows:

$$\begin{aligned} \frac{\partial R_{tot}^{OPS}}{\partial b_1} &= (1-\lambda)\frac{P_r |h_{R1}|^2}{\ln 2\left(\sigma^2 + (1-\rho)b_1 P_r |h_{R1}|^2\right)} - (1-\lambda)\frac{P_r |h_{R2}|^2}{\ln 2\left(\sigma^2 + (1-\rho)b_1 P_r |h_{R2}|^2\right)} \\ &= \frac{1-\lambda}{\ln 2}\left(\left(1/\left(\sigma^2/P_r |h_{R1}|^2\right) + (1-\rho)b_1\right) - \frac{1}{\sigma^2/P_r |h_{R2}|^2 + (1-\rho)b_1}\right). \end{aligned} \tag{26}$$

Since $|h_{R1}|^2 > |h_{R2}|^2$, $\sigma^2/|h_{R1}|^2 < \sigma^2/|h_{R2}|^2$, and $\partial R_{tot}^{OPS}/\partial b_1 > 0$, so R_{tot}^{OPS} is a monotonically increasing function of b_1, and the objective function takes the maximum value when b_1 is maximum. Similarly, the monotonicity of R_{tot}^{TS} in TS strategy also exists.

According to $R_{1\longrightarrow 2} \geq r_{th}$ in SP2, the constraint on b_1 can be obtained as follows:

$$b_1^{OPS} \leq \frac{P_r |h_{R1}|^2 - \sigma^2 R_{th}^{OPS}}{(1-\rho)\left(1 + R_{th}^{OPS}\right)P_r |h_{R1}|^2}. \tag{27}$$

Therefore, the optimal values of b_1 in the *TS* and *OPS* strategies are given by

$$\begin{aligned} b_1^{TS*} &= \min\left(\frac{P_r |h_{R1}|^2 - \sigma_1^2 R_{th}^{TS}}{\left(1 + R_{th}^{TS}\right)P_r |h_{R1}|^2}, 0.5\right), \\ b_1^{OPS*} &= \min\left(\frac{P_r |h_{R1}|^2 - \sigma_1^2 R_{th}^{OPS}}{(1-\rho)\left(1 + R_{th}^{OPS}\right)P_r |h_{R1}|^2}, 0.5\right). \end{aligned} \tag{28}$$

3.3. Optimization of Partition Coefficient. For the TS strategy, SP3 is a univariate optimization problem about λ, and for the OPS strategy, SP3 is a two-variable joint optimization problem about ρ and λ. Referring to the process of solving the optimal transmission power in this paper, this paper also

applies the Dinkelbach algorithm to the suboptimization problem SP3, and equation (16) can be converted into the following expression:

$$\begin{aligned}
&\max_{\rho,\lambda} F_U(\rho,\lambda) - uF_L(\rho,\lambda)\\
&TS: \frac{p_s}{4\eta P_r\left(\left|h_{R1}\right|^2+\left|h_{R2}\right|^2\right)+P_s} \le \lambda \le \min\left(1-\frac{2r_{th}}{\log_2\left(1+\left(b_2P_r\left|h_{R1}\right|^2/\sigma^2+b_1P_r\left|h_{R1}\right|^2\right)\right)}, 1-\frac{2i_{th}}{\log_2\left(1+P_t\left|h_{PP}\right|^2/P_r\left|h_{RP}\right|^2+\sigma_P^2\right)}\right),\\
&OPS: \frac{1-\lambda}{2}\log_2\left(1+\frac{(1-\rho)b_2P_r\left|h_{R1}\right|^2}{\sigma^2+(1-\rho)b_1P_r\left|h_{R1}\right|^2}\right) \ge r_{th}\\
&\left(\frac{4\lambda}{1-\lambda}+2\rho\right)\eta P_r\left(\left|h_{R1}\right|^2+\left|h_{R2}\right|^2\right) \ge P_s\\
&0 \le \rho \le 1, 0 \le \lambda \le 1-\frac{2i_{th}}{\log_2\left(1+P_t\left|h_{PP}\right|^2/P_r\left|h_{RP}\right|^2+\sigma_P^2\right)},
\end{aligned} \tag{29}$$

where $F_U(\rho,\lambda) = R_{tot}$, $F_L(\rho,\lambda) = E_{tot}$, and $u = F_U(\rho,\lambda)/F_L(\rho,\lambda)$.

The specific steps for applying Dinkelbach algorithm in this section are similar to Table 2, $u^{(n)} = F_U(\rho^{(n-1)}, \lambda^{(n-1)})/F_L(\rho^{(n-1)}, \lambda^{(n-1)})$, and are not given here. The proof process of convergence is also given above and the proof process here is similar to it, so it will not be repeated.

Genetic algorithm can solve multivariate optimization problems such as equation (29). This paper uses genetic algorithms to solve these two types of problems. The steps of using genetic algorithm to solve the optimization problem of partition coefficients are as follows. First, M random numbers are generated within the constraint interval satisfied by the partition coefficients of the TS and OPS strategies given in equation (29), and they are converted into a series of "chromosomes" by binary coding. These randomly generated chromosomes are composed of individuals' initial population. Second, let the objective function in SP3 be the fitness function for evaluating the chromosomes, select the highest fitness individual as the best individual, and select M/2 pairs of maternal chromosomes according to the ratio of the fitness of each chromosome to the total fitness of all chromosomes in the population. Third, we randomly select a codeword on the M/2 pair of maternal chromosomes, perform crossover and mutation operations based on the crossover probability p_c and mutation probability p_m to generate M new individuals to form a new population, and update the optimal individual according to the individual fitness in the new population. Crossover is the exchange of codewords corresponding to two chromosomes, and mutation is negation of the codeword. Repeat the above process until the number of iterations reaches the preset algebra G, and the optimal individual at this time is the optimal solution of SP3. The specific implementation process is shown in Table 3.

3.4. Alternate Iteration Algorithm for Joint Optimization. After solving the three suboptimization problems, this paper uses an alternating iterative algorithm to jointly optimize the optimal values of the three suboptimization problems. The specific steps are shown in Table 4.

It is also provable that the energy efficiency η_{EE} increases in each iteration shown in Table 4 and the convergence of the complete algorithm exists. In each iteration, since the Dinkelbach algorithm is used to solve the transmission power problem and the partition coefficient problem, its convergence has been proved above, and the optimal energy efficiency obtained after solving the optimal transmission power is taken as the initial energy efficiency for solving the optimal partition coefficient, and the objective function is a monotonically increasing function of b_1, which ensures that the value of η_{EE} will increase after each iteration.

In addition, Proposition 2 has proved that the objective function in the conversion form equation (21) of SP1 is a concave function about P_r. The local optimum of the unimodal function is the global optimal value; the objective function of SP2 is the monotone increasing function of b_1; the global optimal solution is at the endpoint; the solution method of SP3 is genetic algorithm, it is a global optimization algorithm [25], so the joint optimal energy efficiency optimization algorithm in this paper can guarantee the global optimality of the obtained solution.

Table 3: Genetic algorithm of optimal partition coefficient.

Algorithm: genetic algorithm with optimal partition coefficient
1. Initialize the remaining variables and constant terms $\eta = 80\%$, $b_1 = 0.5$, $P_r = 1$, $T = 1$.
2. Set the number of individuals in the genetic algorithm population M, maximum evolution algebra G, cross probability P_c, mutation probability P_m, initial algebra $g = 1$.
3. Randomly generate M individuals who meet the constraints, calculate the fitness of the initial population according to the objective function and select the individual with the highest fitness as the best individual.
4. While $g < G+1$:
5. Select M/2 to cross the mother chromosomes according to the probability of crossing to generate M new individuals,
6. Make these M new individuals mutate according to the set mutation probability,
7. Let the M chromosomes be a new population and update the most adaptive individual in the population,
8. Let $g = g + 1$.
9. The best individual found is the segmentation coefficients ρ^* and λ^* that satisfy the maximum energy efficiency

Table 4: Joint optimal energy efficiency optimization algorithm.

Algorithm: Joint optimal energy efficiency optimization algorithm
1. Initialize the remaining variables and constant terms $\eta = 80\%$, $b_1^{(1)} = 0.5$, $\lambda_{TS}^{(1)} = 0.3$, $\lambda_{OPS}^{(1)} = 0.2$, $\rho_{OPS}^{(1)} = 0.5$, $T = 1$ and calculate $\eta_{EE}(1)$
2. Let $i = 1$, $\eta_{EE}(0) = \eta_{EE}(1) - \kappa$.
3. While $\lvert\eta_{EE}(i) - \eta_{EE}(i-1)\rvert \geq \kappa$:
4. Let $i = i + 1$,
5. Let $q^{(0)} = \eta_{EE}^{(i-1)}$, substitute the remaining variables $b_1^{(i-1)}$, $\lambda^{(i-1)}$ and $\rho^{(i-1)}$ to solve the optimization problem (25) to obtain $P_r^{(i)}$ and $q_{(i)}^*$ according to Tables 2 and 1.
6. Let $u^{(0)} = q_{(i)}^*$, substitute the remaining variables $b_1^{(i-1)}$ and $P_r^{(i)}$ to solve the optimization problem (28) to obtain $\lambda^{(i)}$, $\rho^{(i)}$ and u_i^* according to Tables 3 and 2 with the iteration conditions replaced with $u^{(n)} = F_U(\rho^{(n-1)}, \lambda^{(n-1)})/F_L(\rho^{(n-1)}, \lambda^{(n-1)})$.
7. Substitute $\lambda^{(i)}$, $\rho^{(i)}$ and $P_r^{(i)}$ into equation (28) to obtain $b_1^{(i)}$;
8. Calculate $\eta_{EE}^{(i)}$ according $b_1^{(i)}$, $\lambda^{(i)}$, $\rho^{(i)}$ and $P_r^{(i)}$;
9. End and get the best P_r, b_1, λ, ρ and η_{EE}.

This paper also provides the complexity analysis of the joint energy efficiency optimization algorithm. The solution process of SP1 and SP3 both use the Dinkelbach method to convert the objective function into a subtraction form; the computational complexity for the Dinkelbach method-based algorithm with stopping criteria ε is $O(\log\varepsilon^{-1})$ [24]. Moreover, we have proved that the objective function of the subtraction form in SP1 is a concave function; the computational complexity of solving the concave function is $O(\log\varepsilon^{-1})$ [26], where ε is the error tolerance for algorithm termination. The optimization process of the NOMA coefficient in SP2 only requires the partial derivative of b_1 for the objective function, whose computational complexity is $O(1)$. The solution process of SP3 employs genetic algorithm; the computational complexity of the genetic algorithm is $O(G \times M \times N)$, which is related to its maximum evolutionary algebra G, the number of individuals in the population M, and the number of variables N [25]. The joint energy efficiency optimization algorithm in this paper nests the Dinkelbach algorithm twice in each iteration, including the golden section method and the genetic algorithm, so the overall computational complexity is $O(\log\kappa^{-1}\log\varepsilon^{-1}(\log\delta^{-1} + G \times M \times N))$, κ, ε, and δ are the error tolerance of the joint energy efficiency optimization algorithm, Dinkelbach algorithm, and golden section method, respectively.

4. Numerical Results

This paper simulates the proposed energy efficiency optimization algorithm with the OPS strategy so that to analyze and compare the system performance of the energy efficiency optimization algorithm of the PS and TS strategy; the calculation of the optimal energy efficiency of the PS strategy comes from the algorithm in [19]. The simulated system model is shown in Figure 1. The parameters are set as follows: $\eta = 80\%$, $P_l = 20dBm$, $P_t = 30dBm$, $i_{th} = 0.1bit/s/\text{Hz}$, $r_{th} = 0.2bit/s/\text{Hz}$, and $T = 1$ [19]. The channel gain between the two-way relay and the secondary user is a random variable obeying the complex Gaussian distribution, namely, $h_{Ri} \sim CN(0, 1/d_i^{\alpha})$ with the average path loss $\alpha = 2$ [19, 27]. d_i is the distance from the secondary user to the two-way relay TWR, and $d_1 = d_3 = 2$ m and $d_2 = d_4 = 10$ m [19].

Figure 4 shows the energy efficiency of the three energy harvesting strategies at different user power thresholds P_s. It can be seen from the figure that the energy efficiency of the three harvesting strategies decreases as P_s increases. This is because the increase of P_s indicates that the system needs to allocate more resources to complete energy harvesting, so resources allocated for information transmission are correspondingly reduced, resulting in a reduction in energy efficiency. The energy efficiency of the OPS strategy is better than the other two strategies. According to the system model analysis of the OPS strategy, OPS can simultaneously control the two partition coefficients of time and power and regulate the ratio of collected energy and information transmission, which is more flexible than the other two strategies so that it can get the highest energy efficiency.

Figure 5 shows the energy efficiency of the three energy harvesting strategies when the distance between the near

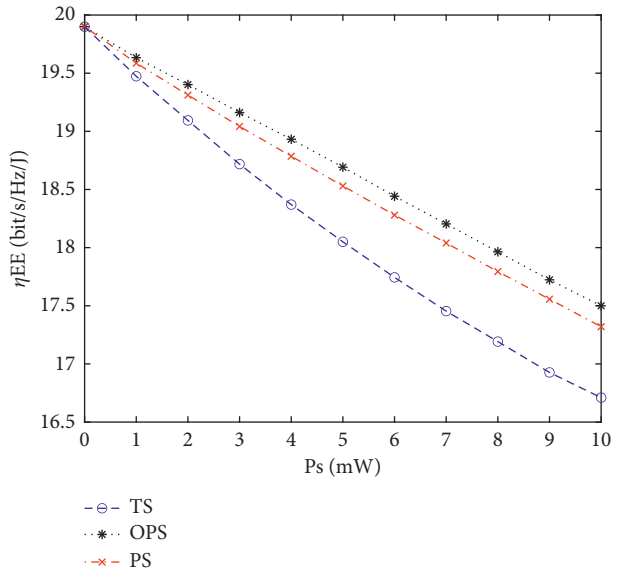

Figure 4: The energy efficiency vs. secondary user power threshold.

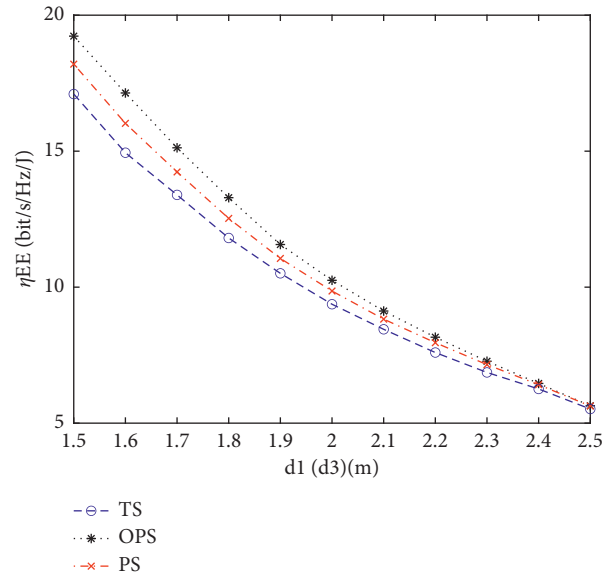

Figure 5: The energy efficiency vs. the distance between the near user and TWR.

user and the relay is different. The distance between the remote user and the relay is the same, that is, $d_2 = d_4 = 10$ m. It can be seen from the figure that the energy efficiency of the three collection strategies decreases with the increase of d_1 and d_3. This is because as the distance between the near user and the relay increases, the information rate of the secondary user decreases and the demand for energy collection increases, resulting in energy efficiency decreasing. The energy efficiency of the OPS strategy is better than the other two strategies which is because, with the increase of the distance between the near user and the relay, the OPS strategy can simultaneously control the time division and power partition to regulate the ratio of collected energy and information transmission. With the increase of d_1, the energy efficiency difference of the three strategies is gradually narrowing, which indicates that the energy efficiency impact of the three strategies is gradually decreasing.

Figure 6 shows the energy consumption of the three strategies at different user power thresholds P_s. It can be seen from the figure that the energy consumption E_{tot} of the three strategies rises with the increase of the user power limit P_s, which is because as the power limit of secondary users increases, the resource requirements for harvesting energy increase, and the relay power and the partition coefficient increase correspondingly, leading to an increase in energy consumption. The OPS strategy consumes less energy than the PS and TS strategies because the OPS strategy can control both time division and power division to ensure that the system completes the communication process with the lowest energy requirements.

Figure 7 shows the system capacity of the OPS strategy with different P_s at $\eta = 0.8$ and $\eta = 0.6$. It can be seen from the figure that the system capacity of the OPS strategy decreases with the increase of P_s. As P_s increases, the system needs to allocate more resources to harvest energy, and the resources allocated for information transmission are correspondingly reduced, at the same time, the decrease in the

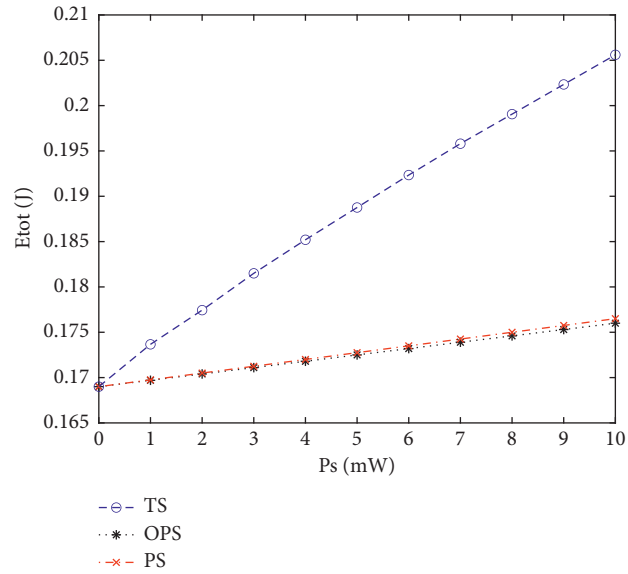

Figure 6: The energy consumption vs. secondary user power threshold.

information rate of the secondary users results in a decrease in system capacity. The system capacity at $\eta = 0.8$ is higher than the system capacity at $\eta = 0.6$ because higher energy collection efficiency means lower energy requirements, OPS strategy can regulate more resources for information transmission, and the corresponding system capacity would be higher.

Figure 8 shows the system capacity of the OPS strategy when relay power $P_r = 0.2W$ and $P_r = 0.1W$ at different b_1. It can be seen from the figure that the system capacity of the OPS strategy increases with the increase of b_1, which is because the near user has a higher channel gain than the far user, increasing

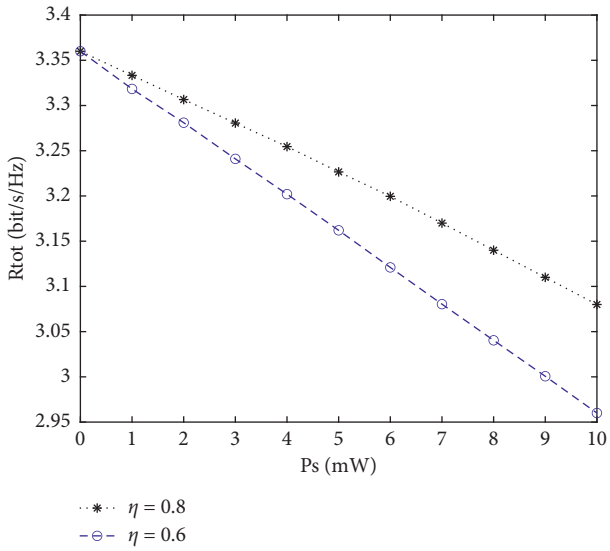

Figure 7: The sum rate vs. secondary user power threshold when $\eta = 0.8$ and $\eta = 0.6$.

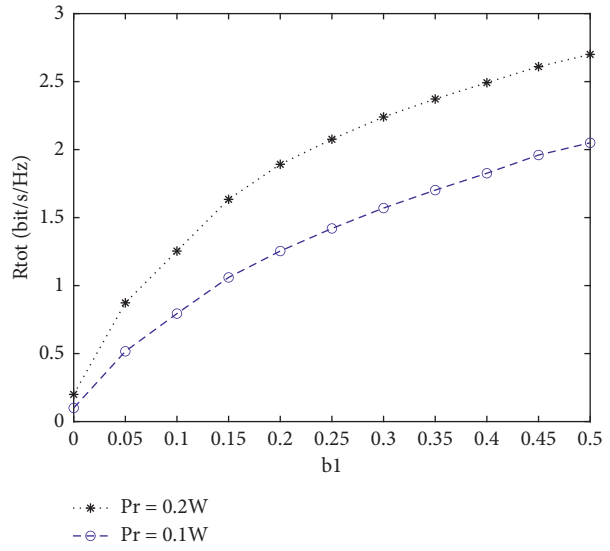

Figure 8: The sum rate vs. NOMA coefficient when $P_r = 0.2W$ and $P_r = 0.1W$.

the NOMA power allocation coefficient that TWR forwards to the near user will significantly increase the information rate of the near user, resulting in a corresponding increase in system capacity. The system capacity at $P_r = 0.2W$ is higher than the system capacity at $P_r = 0.1W$ because increasing the relay power increases the signal-to-interference-and-noise ratio of the secondary user's received signal, and the increase in the information rate causes the system capacity to increase.

5. Conclusion

This paper proposes a system energy efficiency optimization algorithm using the OPS strategy for a two-way relay CR-NOMA system based on SWIPT. The system capacity expressions with the TS strategy and the OPS strategy are derived, respectively. Under the constraints of harvested energy and quality of service, an optimization problem with the goal of maximizing energy efficiency is constructed. The objective function is a multiobjective optimized NP-Hard problem. In this paper, the original problem is transformed into three subproblems about relay power, NOMA coefficient, and segmentation coefficient, which are solved by the golden section algorithm, the monotonicity determination method of the function, and the genetic algorithm; then, the solutions of three subproblems are jointly optimized by alternating iterative algorithm. The simulation results show that compared with the PS and TS strategies, the OPS strategy can significantly improve the transmission energy efficiency of the system. Since the OPS strategy can control time division and power division at the same time, thereby ensuring that the system completes the communication process with the lowest energy requirements, OPS strategy is better than PS and TS strategy when the power limit of different users and the distance between the near user and the relay are different.

Data Availability

The data (figures) used to support the findings of this study are included within the article. Further details can be provided upon request.

Conflicts of Interest

The authors declare that they have no conflicts of interest.

Acknowledgments

The work of Zhen Wang and Qi Zhu was supported by the National Natural Science Foundation of China under Grant nos. 61971239 and 61631020.

References

[1] Y. Zhang, P. Chowdhury, M. Tornatore, and B. Mukherjee, "Energy efficiency in telecom optical networks," *IEEE Communications Surveys & Tutorials*, vol. 12, no. 4, pp. 441–458, 2010.

[2] G. He, L. Li, X. Li, W. Chen, L. Yang, and Z. Han, "Secrecy sum rate maximization in NOMA systems with wireless information and power transfer," in *Proceedings of the 2017 9th International Conference on Wireless Communications and Signal Processing (WCSP)*, pp. 1–6, Nanjing, China, October 2017.

[3] I. Krikidis, "Simultaneous wireless information and power transfer in modern communication systems," *Communications Magazine, IEEE*, vol. 52, no. 11, pp. 104–110, 2014.

[4] A. A. Nasir, X. Zhou, S. Durrani, and R. A. Kennedy, "Relaying protocols for wireless energy harvesting and information processing," *IEEE Transactions on Wireless Communications*, vol. 12, no. 7, pp. 3622–3636, 2013.

[5] A. A. Nasir, X. Zhou, S. Durrani, and R. A. Kennedy, "Wireless-powered relays in cooperative communications: time-switching relaying protocols and throughput analysis,"

IEEE Transactions on Communications, vol. 63, no. 5, pp. 1607–1622, 2015.

[6] X. Zhou, R. Zhang, and C. K. Ho, "Wireless information and power transfer: architecture design and rate-energy tradeoff," *IEEE Transactions on Communications*, vol. 61, no. 11, pp. 4754–4767, 2013.

[7] K. Huang and E. Larsson, "Simultaneous information and power transfer for broadband wireless systems," *IEEE Transactions on Signal Processing*, vol. 61, no. 23, pp. 5972–5986, 2013.

[8] X. Zhou, R. Zhang, and C. K. Ho, "Wireless information and power transfer in multiuser OFDM systems," *IEEE Transactions on Wireless Communications*, vol. 13, no. 4, pp. 2282–2294, 2014.

[9] S. K. Zaidi, S. F. Hasan, and X. Gui, "Time switching based relaying for coordinated transmission using NOMA," in *Proceedings of the 2018 Eleventh International Conference on Mobile Computing and Ubiquitous Network (ICMU)*, pp. 1–5, Auckland, New Zealand, October 2018.

[10] L. Bariah, S. Muhaidat, and A. Al-Dweik, "Error probability analysis of NOMA-based relay networks with SWIPT," *IEEE Communications Letters*, vol. 23, no. 7, pp. 1223–1226, 2019.

[11] J. Tang, Y. Yu, and M. Liu, "Joint power allocation and splitting control for SWIPT-enabled NOMA systems," *IEEE Transactions on Wireless Communications*, vol. 19, no. 1, pp. 120–133, 2020.

[12] M. Hedayati and I. Kim, "On the performance of NOMA in the two-user SWIPT system," *IEEE Transactions on Vehicular Technology*, vol. 67, no. 11, pp. 11258–11263, 2018.

[13] J. Tang, "Energy efficiency optimization for NOMA with SWIPT," *IEEE Journal of Selected Topics in Signal Processing*, vol. 13, no. 3, pp. 452–466, 2019.

[14] Z. Chang, "Energy-efficient and secure resource allocation for multiple-antenna NOMA with wireless power transfer," *IEEE Transactions on Green Communications and Networking*, vol. 2, no. 4, pp. 1059–1071, 2018.

[15] F. Jameel, *Secrecy Analysis and Learning-Based Optimization of Cooperative NOMA SWIPT Systems*, IEEE ICC, Shanghai, China, 2019.

[16] Y. Yu, Z. Yang, Y. Wu, J. A. Hussein, W. Jia, and Z. Dong, "Outage performance of NOMA in cooperative cognitive radio networks with SWIPT," *IEEE Access*, vol. 7, pp. 117308–117317, 2019.

[17] Z. Yang, Z. Ding, P. Fan, and N. Al-Dhahir, "The impact of power allocation on cooperative non-orthogonal multiple access networks with SWIPT," *IEEE Transactions on Wireless Communications*, vol. 16, no. 7, pp. 4332–4343, 2017.

[18] X. Wang, "Energy efficiency optimization for NOMA-based cognitive radio with energy harvesting," *IEEE Access*, vol. 7, pp. 139172–139180, 2019.

[19] W. Zhao, R. She, and H. Bao, "Energy efficiency maximization for two-way relay assisted CR-NOMA system based on SWIPT," *IEEE Access*, vol. 7, pp. 72062–72071, 2019.

[20] E. Boshkovska, D. W. K. Ng, N. Zlatanov, and R. Schober, "Practical non-linear energy harvesting model and resource allocation for SWIPT systems," *IEEE Communications Letters*, vol. 19, no. 12, pp. 2082–2085, 2015.

[21] B. Clerckx, R. Zhang, R. Schober, D. W. K. Ng, D. I. Kim, and H. V. Poor, "Fundamentals of wireless information and power transfer: from RF energy harvester models to signal and system designs," *IEEE Journal on Selected Areas in Communications*, vol. 37, no. 1, pp. 4–33, 2019.

[22] S. Boyd and L. Vandenberghe, *Convex Optimization*, Cambridge University Press, Cambridge, UK, 2004.

[23] Z. Chang, "Energy-efficient resource allocation and user scheduling for collaborative mobile clouds with hybrid receivers," *IEEE Transactions on Vehicular Technology*, vol. 65, no. 12, pp. 9834–9846, 2016.

[24] W. Dinkelbach, "On nonlinear fractional programming," *Management Science*, vol. 13, no. 7, pp. 492–498, 1967.

[25] P. Ponterosso and D. S. J. Fox, "Optimization of reinforced soil embankments by genetic algorithm," *International Journal for Numerical & Analytical Methods in Geomechanics*, vol. 24, no. 4, pp. 425–433, 2000.

[26] J. J. M. Paul and H. Calamai, "Projected gradient methods for linearly constrained problems," *Mathematical Programming*, vol. 39, no. 1, pp. 93–116, 1987.

[27] X. Yue, Y. Liu, S. Kang, A. Nallanathan, and Y. Chen, "Modeling and analysis of two-way relay non-orthogonal multiple access systems," *IEEE Transactions on Communications*, vol. 66, no. 9, pp. 3784–3796, 2018.